RSC Advances

PAPER

View Article Online
View Journal | View Issue

Cite this: *RSC Adv.*, 2017, **7**, 28606

Modulating photo-luminescence of Au_2Cu_6 nanoclusters *via* ligand-engineering†

Xi Kang, Xiaowu Li,* Haizhu Yu, Ying Lv, Guodong Sun, Yangfeng Li, Shuxin Wang and Manzhou Zhu*

Received 27th April 2017
Accepted 25th May 2017

DOI: 10.1039/c7ra04743f

rsc.li/rsc-advances

In this work, the luminescence of Au_2Cu_6 nanoclusters was controlled by tailoring the ligand to metal charge transfer *via* engineering the phosphine ligands with electron-donating or -withdrawing substituents. The fluorescence intensity was significantly enhanced from the Au_2Cu_6 nanocluster with $P(Ph-F)_3$ ligands (quantum yield QY = 5.7%) to that with $P(Ph-OMe)_3$ ligands (QY = 17.7%). In addition, the fluorescence of Au_2Cu_6 protected by $P(Ph-OMe)_3$ slightly red-shifts compared to that of Au_2Cu_6 protected by $P(Ph-F)_3$, which is similar to the trends of UV-vis spectra tendency.

Metal nanoclusters (NCs) with precise atomic number and well-defined composition (structure) have attracted intensive research interest owing to their highly promising applications in optics, catalysis and electrochemistry.[1–11] In this context, photo-luminescence (PL) represents one of the most attractive properties of the metal NCs.[1,4,6,8,12] Thanks to the advantages such as low toxicity, great photo-stability and high biocompatibility, the fluorescent NCs have recently become highly promising nanomaterials in phototherapy, cell labeling and biosensing.[6,8,13,14] Thus far, several fluorescent NCs have been successfully synthesized.[13–23] Unfortunately, their practical applications have been limited due to the significantly lower quantum yield (QY) compared to the typical fluorescent nanomaterials (*e.g.*, quantum dots).[1,15] To this end, an efficient strategy to enhance the QY of weakly fluorescent NCs is highly desirable.

In the past decades, two main strategies (*i.e.*, foreign-metal-doping[15,18,19] and ligand-engineering strategies[15–17,22]) have been developed to enhance the fluorescence of NCs. For instance, Bakr *et al.* observed a 26-fold PL QY enhancement on Ag_{29} NC when doped with the central Au atom.[19b] In addition, Wu and coworkers reported that the fluorescence intensity of Au_{24} NC increased with an increase in the electron-donating ability of the ligand.[14] In recent years, the ligand-engineering strategy has attracted increasing interest.[15–17,22] As the electronic structures of the organic ligands are essentially different from those of the metal atoms, the mechanistic understanding on the structure (composition)–fluorescence correlation could be more achievable.[14,17c] Additionally, with the structure–fluorescence relationships in hand, the target NCs with stronger PL could be easily prepared due to the synthetic similarities of NCs protected by different organic ligands.

In our recent study, the $Au_2Cu_6(S\text{-}Adm)_6(PPh_2Py)_2$ (where S-Adm = 1-adamantanethiol) NC with high fluorescence (QY = 11.7%) was synthesized *via* the aggregation-induced-emission method.[18c] The DFT calculations indicate that the fluorescence corresponds to the LUMO–HOMO transition, and is mainly caused by the charge transfer between the aromatic groups on the phosphine ligand and copper atoms. In other words, the luminescence originated from ligand to metal charge transfer (LMCT).[18c] Inspired by these conclusions, we tried to tailor the PL of Au_2Cu_6 NCs by engineering the phosphine ligands *via* functionalizing the aromatic group with electron-donating groups (EDGs) or electron-withdrawing substituents (EWGs). As summarized in Scheme 1, the EDG will hopefully strengthen the LMCT process to enhance the fluorescence. On

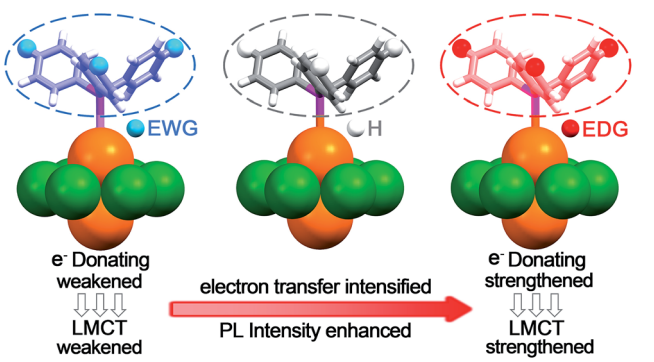

Scheme 1 The illustrations of decreased LMCT and fluorescence induced by EWG; contrastive LMCT (PPh_3); enhanced LMCT and fluorescence induced by EDG.

Department of Chemistry, Center for Atomic Engineering of Advanced Materials, Anhui Province Key Laboratory of Chemistry for Inorganic/Organic Hybrid Functionalized Materials, Anhui University, Hefei, Anhui 230601, China. E-mail: xiaowuli2006@hotmail.com; zmz@ahu.edu.cn

† Electronic supplementary information (ESI) available: Synthesis, characterization details and X-ray crystallographic (CIF) data. CCDC 1539336 & 1539376. For ESI and crystallographic data in CIF or other electronic format see DOI: 10.1039/c7ra04743f

the contrary, the LMCT and fluorescence could be significantly weakened when the phosphine ligand is relatively electron-deficient (in the presence of EWG).

Herein, we reported the PL modulation of Au_2Cu_6 NC systems *via* engineering the phosphine ligands with the electronic effect of the substituents. The structures and compositions of the $Au_2Cu_6(S\text{-}Adm)_6(PR_3)_2$ (R = Ph–OMe for **Au_2Cu_6-1**; R = Ph for **Au_2Cu_6-2**; and R = Ph–F for **Au_2Cu_6-3**) NCs were verified by single crystal X-ray diffraction (SC-XRD), thermogravimetric analysis (TGA), inductively coupled plasma (ICP) and X-ray photoelectric spectroscopy (XPS) measurements. According to these characterizations, all the NCs share the same framework with the previously reported $Au_2Cu_6(S\text{-}Adm)_6(PPh_2Py)_2$ NC. Compared with **Au_2Cu_6-2** (QY = 12.2%), **Au_2Cu_6-1** with EDGs exhibits enhanced PL (QY = 17.7%), while **Au_2Cu_6-3** with EWGs shows weaker luminescence (QY = 5.7%). In addition, the emission peak on the PL spectra slightly red-shifts from **Au_2Cu_6-1** to **Au_2Cu_6-2** and **Au_2Cu_6-3**, consistent with the variation tendency in UV-vis spectra of different Au_2Cu_6 systems.

The aforementioned three Au_2Cu_6 NCs were prepared by the similar procedures with our previous study[18c] (see ESI† for details). Specifically, CuCl was dissolved in the mixture of acetonitrile and methanol, and AdmSH dissolved in toluene was then added to the solution. The overall solution was vigorously stirred for 15 min. Then, $Au(PR_3)Cl$ (R = Ph–OMe, Ph or Ph–F) in toluene and $NaBH_4$ in ice-cold water were added dropwise to the flask simultaneously under vigorous stirring. The reaction was aged for 60 h under N_2 atmosphere. Afterwards, the products were centrifuged to obtain the solid, which was then washed several times with toluene for further characterizations.

According to the SC-XRD characterization, the composition and total structures of the as-prepared **Au_2Cu_6-2** and **Au_2Cu_6-3** are similar with the overall framework of previously reported $Au_2Cu_6(S\text{-}Adm)_6(PPh_2Py)_2$ (Fig. S1 and S2†). However, the crystal structure of **Au_2Cu_6-1** failed to be obtained because of the relatively weak stability. Thus, TGA, XPS and ICP measurements were performed to ascertain the composition of **Au_2Cu_6-1**. The weight loss of 69.15% (Fig. S3–S5†) is consistent with the theoretical value (cal. 68.79%) of AdmSH and $(Ph\text{–}OMe)_3P$ ligands in **Au_2Cu_6-1**. In addition, the XPS and ICP results suggest that the metallic ratio of Au and Cu in **Au_2Cu_6-1** was 1 : 3 (Fig. S6–S8 and Table S3†). Combining the TGA, XPS and ICP results with the almost identical UV-vis spectra (*vide infra*), we conclude that the structure of **Au_2Cu_6-1** is similar to those of the other Au_2Cu_6 NCs. In other words, all these Au_2Cu_6 structures follow the same framework (*i.e.*, $Au_2(PR_3)_2$ axis surrounded by six Cu(S-Adm) complexes on the equatorial plane) no matter whether the electron-donating –OMe or electron-withdrawing –F substituents are introduced.

Although the point groups of **Au_2Cu_6-2** and **Au_2Cu_6-3** NCs are both D_{3d}, the crystal system in space group of **Au_2Cu_6-2** is trigonal, unlike the triclinic arrangement of **Au_2Cu_6-3** (see Tables S1 and S2 for more details, ESI†). In addition, **Au_2Cu_6-2** and **Au_2Cu_6-3** exhibit some distinct structural parameters. As shown in Fig. 1, depending on the relative location around the equatorial plane, the S atoms in each NC could be categorized

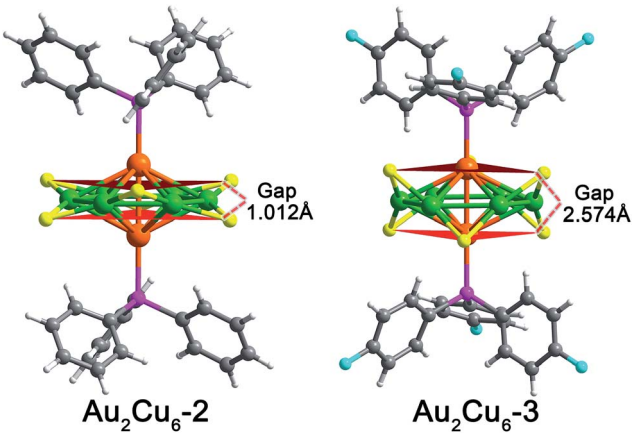

Fig. 1 Crystal structures of Au_2Cu_6 NCs protected by PPh_3 or $P(Ph\text{–}F)_3$ ligands. Color legends: orange, Au; green, Cu; yellow, S; purple, P; cyan, F; gray, C and light gray, H. For clarity, the C and H atoms on the thiol ligands are omitted.

into two groups. The Au–Cu–S angles in **Au_2Cu_6-3** are 85° (with upward S atoms) and 115° (with downward S atoms). This related angles in **Au_2Cu_6-2** are significantly larger (103° or 117°). Meanwhile, the gap between the two planes constituted by the two groups of S atoms (in red planes) is 1.102 Å in **Au_2Cu_6-2**, while the gap is remarkably larger in **Au_2Cu_6-3** (2.574 Å). The lower steric hindrance between the different thiol groups in **Au_2Cu_6-3** results in a more regular thiolate ligands configuration (Fig. S9†). In view of the electronic effect, the weaker electron donating ability of $P(Ph\text{–}F)_3$ results in inferior electron transfer from phosphine ligands to metallic core in **Au_2Cu_6-3** compared to **Au_2Cu_6-2**. Accordingly, the interaction between Au and P is relatively weaker in **Au_2Cu_6-3**, and thus the Au–P bond distances **Au_2Cu_6-3** (2.336 Å in average) are slightly longer compared with those in **Au_2Cu_6-2** (2.325 Å in average).

The UV-vis spectra of these three Au_2Cu_6 NCs were compared to illustrate the ligand effect on the optical adsorption. As

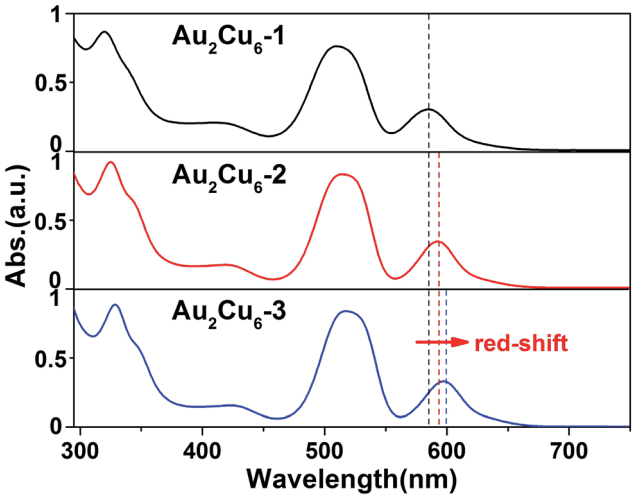

Fig. 2 UV-vis spectra of **Au_2Cu_6-1**, **Au_2Cu_6-2** and **Au_2Cu_6-3** NCs. The final characteristic absorption peak was red-shifted from 585 nm to 594 nm and 600 nm.

shown in Fig. 2, no obvious shifts occur on the front three peaks (*i.e.*, 325, 420 and 515 nm). In contrary, the final characteristic absorption peak slightly red-shifts from 585 nm of **Au_2Cu_6-1** to 600 nm of **Au_2Cu_6-3** (cal. 15 nm). Therefore, the almost maintained spectra validate the similar framework in these Au_2Cu_6 NCs, and the similar HOMO–LUMO gap suggests that the similar transition occurs in all these Au_2Cu_6 NCs.[18c] Nonetheless, the alternation of the substituents with different electronic effect induces the slight difference in the optical property. The EDGs tend to elevate both the HOMO and LUMO energies, and the HOMO–LUMO gap is enlarged because LUMO is more sensitive to the electronic effect of the substituents.[24,25] By contrast, both HOMO and LUMO energies of the NCs reduce when the EWGs are introduced, and the significantly lowered LUMO energy (compared to that of HOMO energy) results in a reduced HOMO–LUMO gap.[24,25]

The PL spectra of Au_2Cu_6 NCs was characterized to verify the aforementioned inference of electronic effect. Comparing the different fluorescent spectra of Au_2Cu_6 NCs in Fig. 3, we find that **Au_2Cu_6-1** shows the strongest fluorescence and **Au_2Cu_6-3** shows the weakest one. Specifically, the QY of **Au_2Cu_6-2** was 12.2%. The QY was enhanced to 17.7% when the more electron donating $P(Ph–OMe)_3$ ligands (*i.e.*, **Au_2Cu_6-1**) were used. By contrast, the **Au_2Cu_6-3** protected by the less electron donating $P(Ph–F)_3$ ligands shows a lower QY (5.7%). Consequently, the **Au_2Cu_6-1** exhibits a brighter fluorescent response under UV light irradiation compared with the other Au_2Cu_6 NCs (Fig. 3, insets). In addition, the PL peak of **Au_2Cu_6-1** centered at 656 nm slightly red-shifts to 660 nm in **Au_2Cu_6-2** and 667 nm in **Au_2Cu_6-3**. The relatively smaller LUMO–HOMO gap induced by the electronic effect of the substituents accounts for the luminescence red-shift. This observation also correlates well with the similar red-shift tendency in the UV-vis spectra.

The relaxation dynamics of the three Au_2Cu_6 NCs were analysed (Fig. S10†). The time constant of the **Au_2Cu_6-1** NC excited-state decay (about 8.6 μs) due to the LMCT process.[18,19,26,27] When the phosphine ligands were altered to PPh_3 or $P(Ph–F)_3$, the relaxation time constant was found to decrease to 6.4 and 5.4 μs, respectively. It has been discussed above that the replacement of $P(Ph–OMe)_3$ ligands to PPh_3 and $P(Ph–F)_3$ ligands reduced the HOMO–LUMO gap and weakened the LMCT process, which might be the reason of shorter relaxation time constants of **Au_2Cu_6-2** and **Au_2Cu_6-3** NCs.

In summary, the fluorescent intensity of Au_2Cu_6 NCs was controllable tailored by engineering the phosphine ligands with electron-donating (*i.e.*, –OMe) or electron-withdrawing (*i.e.*, –F) substituents. The distinct electronic effect was successfully used to modulate the LMCT process, and then control the fluorescent intensity. When protected by the electron-rich $P(Ph–OMe)_3$ ligand, the Au_2Cu_6 NC exhibits enhanced fluorescence with QY = 17.7% compared with that protected by PPh_3 (QY = 12.2%). On the contrary, the QY was decreased when the Au_2Cu_6 NC is protected by relatively electron-deficient ligands (*i.e.*, $P(Ph–F)_3$). In addition, the PL spectrum of Au_2Cu_6 protected by $P(Ph–F)_3$ displays a slight red-shift compared with other Au_2Cu_6 NCs, which is similar to the observations in UV-vis spectra. This study presents a controllable strategy to enhance the PL of noble metal NCs, and also sheds lights on synthesizing new class of highly fluorescent NCs.

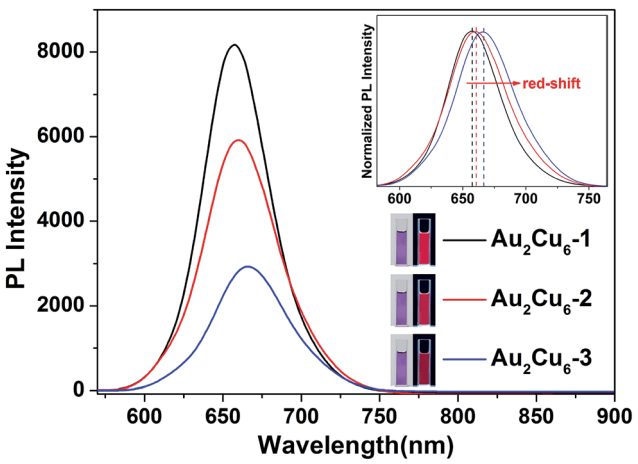

Fig. 3 The spectra on the PL of the Au_2Cu_6-1, Au_2Cu_6-2 and Au_2Cu_6-3 NCs. Insets: the red-shift in normalized PL spectra of these three Au_2Cu_6 NCs; the digital photographs of the corresponding NCs under visible and UV light.

Acknowledgements

We acknowledges financial support by NSFC (21372006, U1532141 & 21631001), the Ministry of Education, the Education Department of Anhui Province, 211 Project of Anhui University.

Notes and references

1 R. Jin, C. Zeng, M. Zhou and Y. Chen, *Chem. Rev.*, 2016, **116**, 10346–10413.
2 P. Liu, R. Qin, G. Fu and N. Zheng, *J. Am. Chem. Soc.*, 2017, **139**, 2122–2131.
3 C. P. Joshi, M. S. Bootharaju and O. M. Bakr, *J. Phys. Chem. Lett.*, 2015, **6**, 3023–3035.
4 N. Goswami, Q. Yao, Z. Luo, J. Li, T. Chen and J. Xie, *J. Phys. Chem. Lett.*, 2016, **7**, 962–975.
5 Z. Lei, X.-K. Wan, S.-F. Yuan, J.-Q. Wang and Q.-M. Wang, *Dalton Trans.*, 2017, **46**, 3427–3434.
6 A. Mathew and T. Pradeep, *Part. Part. Syst. Charact.*, 2014, **31**, 1017–1053.
7 W. Kurashige, Y. Niihori, S. Sharma and Y. Negishi, *J. Phys. Chem. Lett.*, 2014, **5**, 4134–4142.
8 Y. Tao, M. Li, J. Ren and X. Qu, *Chem. Soc. Rev.*, 2015, **44**, 8636–8663.
9 S. Yamazoe, S. Takano, W. Kurashige, T. Yokoyama, K. Nitta, Y. Negishi and T. Tsukuda, *Nat. Commun.*, 2016, **7**, 10414.
10 T. M. Carducci, R. E. Blackwell and R. W. Murray, *J. Am. Chem. Soc.*, 2014, **136**, 11182–11187.
11 A. Dass, S. Theivendran, P. R. Nimmala, C. Kumara, V. R. Jupally, A. Fortunelli, L. Sementa, G. Barcaro, X. Zuo and B. C. Noll, *J. Am. Chem. Soc.*, 2015, **137**, 4610–4613.
12 K. L. D. M. Weerawardene and C. M. Aikens, *J. Am. Chem. Soc.*, 2016, **138**, 11202–11210.

13 X.-D. Zhang, Z. Luo, J. Chen, X. Shen, S. Song, Y. Sun, S. Fan, F. Fan, D. T. Leong and J. Xie, *Adv. Mater.*, 2014, **26**, 4565–4568.

14 Z. Gan, Y. Lin, L. Luo, G. Han, W. Liu, Z. Liu, C. Yao, L. Weng, L. Liao, J. Chen, X. Liu, Y. Luo, C. Wang, S. Wei and Z. Wu, *Angew. Chem., Int. Ed.*, 2016, **55**, 11567–11571.

15 S. Wang, X. Meng, A. Das, T. Li, Y. Song, T. Cao, X. Zhu, M. Zhu and R. Jin, *Angew. Chem., Int. Ed.*, 2014, **53**, 2376–2380.

16 R.-W. Huang, Y.-S. Wei, X.-Y. Dong, X.-H. Wu, C.-X. Du, S.-Q. Zang and T. C. W. Mak, *Nat. Chem.*, 2017, DOI: 10.1038/nchem.2718.

17 (*a*) G. Li, Z. Lei and Q.-M. Wang, *J. Am. Chem. Soc.*, 2010, **132**, 17678–17679; (*b*) Z. Lei, X.-L. Pei, Z.-G. Jiang and Q.-M. Wang, *Angew. Chem., Int. Ed.*, 2014, **53**, 12771–12775; (*c*) X.-Y. Liu, Y. Yang, Z. Lei, Z.-J. Guan and Q.-M. Wang, *Chem. Commun.*, 2016, **52**, 8022–8025.

18 (*a*) X. Kang, M. Zhou, S. Wang, S. Jin, G. Sun, M. Zhu and R. Jin, *Chem. Sci.*, 2017, **8**, 2581–2587; (*b*) X. Kang, L. Xiong, S. Wang, H. Yu, S. Jin, Y. Song, T. Chen, L. Zheng, C. Pan, Y. Pei and M. Zhu, *Chem.–Eur. J.*, 2016, **22**, 17145–17150; (*c*) X. Kang, S. Wang, Y. Song, S. Jin, G. Sun, H. Yu and M. Zhu, *Angew. Chem., Int. Ed.*, 2016, **55**, 3611–3614.

19 (*a*) M. S. Bootharaju, C. P. Joshi, M. R. Parida, O. F. Mohammed and O. M. Bakr, *Angew. Chem., Int. Ed.*, 2016, **55**, 922–926; (*b*) G. Soldan, M. A. Aljuhani, M. S. Bootharaju, L. G. AbdulHalim, M. R. Parida, A.-H. Emwas, O. F. Mohammed and O. M. Bakr, *Angew. Chem., Int. Ed.*, 2016, **55**, 5749–5753.

20 (*a*) Z. Luo, X. Yuan, Y. Yu, Q. Zhang, D. T. Leong, J. Y. Lee and J. Xie, *J. Am. Chem. Soc.*, 2012, **134**, 16662–16670; (*b*) K. Zheng, X. Yuan, K. Kuah, Z. Luo, Q. Yao, Q. Zhang and J. Xie, *Chem. Commun.*, 2015, **51**, 15165–15168; (*c*) Y. Yu, Z. Luo, D. M. Chevrier, D. Tai Leong, P. Zhang, D.-e. Jiang and J. Xie, *J. Am. Chem. Soc.*, 2014, **136**, 1246–1249.

21 Y. Wang, H. Su, L. Ren, S. Malola, S. Lin, B. K. Teo, H. Häkkinen and N. Zheng, *Angew. Chem., Int. Ed.*, 2016, **55**, 15152–15156.

22 Z. Wu and R. Jin, *Nano Lett.*, 2010, **10**, 2568–2573.

23 T. Udayabhaskararao, Y. Sun, N. Goswami, S. K. Pal, K. Balasubramanian and T. Pradeep, *Angew. Chem., Int. Ed.*, 2012, **51**, 2155–2159.

24 L. Sementa, G. Barcaro, O. Baseggio, M. D. Vetta, A. Dass, E. Apra, M. Stener and A. Fortunelli, *J. Phys. Chem. C*, 2017, **121**, 10832–10842.

25 G. Lugo, V. Schwanen, B. Fresch and F. Remacle, *J. Phys. Chem. C*, 2015, **119**, 10969–10980.

26 S. H. Yau, O. Varnavski and T. Goodson, *Acc. Chem. Res.*, 2013, **46**, 1506–1516.

27 M. Pelton, Y. Tang, O. M. Bakr and F. Stellacci, *J. Am. Chem. Soc.*, 2012, **134**, 11856–11859.